25th ABCM International Congress of Mechanical Engineering
October 20-25, 2019, Uberlândia, MG, Brazil

COB-2019-0794
ON THE ACOUSTIC RADIATION OF A 1D PIEZOELECTRIC METASTRUCTURE

Gabriel Konda Rodrigues[1]
Jaime Alberto Mosquera-Sánchez[2]
Carlos De Marqui Jr.[2]
Leopoldo Pisanelli Rodrigues de Oliveira[1a]
[1]Department of Mechanical Engineering, São Carlos School of Engineering, University of São Paulo. Av. Trabalhador Sancarlense, 400, 13566-590 São Carlos, Brazil.
[a]leopro@sc.usp.br.
[2]Department of Aeronautics Engineering, São Carlos School of Engineering, University of São Paulo. Av. João Dagnone, 1100, 13563-120 São Carlos, Brazil.
jamosquera@usp.br.

Abstract. *As sound pollution becomes a serious concern nowadays, engineers and researchers are looking for ways to directly deal with the noise sources for blocking its propagation. In this regard, Acoustic Metamaterials (AMM) constitute an interesting strategy for dealing with sound propagation, once that they are capable of creating a stop band at which mechanical waves cannot propagate, thus reducing transmission and/or noise levels. This paper proposes an acoustic field study and further analyses on the sound transmission loss (STL) through a acoustic metastructure that features piezoelectric-based circuit attachments. It is seen that the electrical attachments provide the mechanical structure with improved, adaptive features, e.g. band gap broadening and multi frequency targeting, which allows the designer to tackle a variety of noises, whose frequency distribution can vary. While vibroacoustic analyses on the radiated sound field are ongoing, the experimental results obtained on the proposed 1D structure demonstrate effective wave propagation blocking at a given frequency bandwidth.*

Keywords: *Smart materials, locally resonant metamaterials, sound transmission loss, piezoelectric shunt circuits.*

1. INTRODUCTION

Resonances are often a problem when dealing with structural dynamic behavior, as it relates to fatigue and failure (in extreme cases), as well as to sound pollution or noise. Both issues are nowadays becoming of paramount importance in machine and system design, since they are related to the overall quality of the product operation, thus driving the degree of conformity between an user and a product. A number of techniques are used to achieve a satisfactory suppression on the structural vibrations, such as increasing the overall damping factor (Douglas and Yang, 1978; Dovstam, 1995), dynamic absorbers (Inman and Singh, 1994), and also active/semi-active control systems (Mosquera-Sánchez *et al.*, 2017; De Oliveira *et al.*, 2008) , amongst others. Metamaterials (MM) are gaining interest in these applications for their so-called unusual physical properties, e.g. negative mass and/or stiffness, as well as by its ability to create frequency bands at which mechanical waves cannot propagate within the main structure.

Currently, there are two known mechanisms that promote those effects, which are the Bragg scattering that is derived from the photonic crystals and rely on destructive interference of the waves, and local resonances that exhibit a similar behavior as a linear tuned vibration absorber (LTVA). The latter metamaterial mechanism constitutes an interesting approach, since locally resonant metamaterials (LRMM) are capable of achieving lower frequencies stop bands as the Bragg-based MM. This is a desirable characteristic for a structure, as the first, high-power structural resonances are located on this bandwidth. In addition, the more prominent acoustical noise content is commonly found in this bandwidth.

Smart materials are not a novelty field. However, their features pose an interesting solution for performance improvement, such as piezoelectric patches, in combination with MM. Some efforts found in the literature show the combination of these areas, mainly focused for mechanical-to-electrical energy harvesting (Li *et al.*, 2016). Unlike these sort of harvesters, smart metamaterials (SMM) are a recent yet very promising strategy for performance increase with possibilities for suppressing broadband vibration.

Therefore, this paper presents an 2D electro-vibroacoustic analysis for an metastructure. Firstly, some modeling insights will be presented for design and simulation of the structural behavior. Then, a vibroacoustic study of the metastructure will be presented with the utilization of both Finite Element (FEM) and Boundary Element Methods (BEM). A

structural analysis were chosen over a wave formulation as non-periodicity can be dealt without penalising the model formulation.

2. MODELING PROCEDURE

This research pursues improved STL capabilities of typical slender structural members in bending motion. Dynamical bending of slender, lightweight structures within the audible frequency range causes the surrounding fluid to oscillate in such a form that acoustic, audible waves are radiated onto the environment. It is widely known that lightweight structures made by lightly damped, homogeneous materials, *e.g.* steel, aluminum, etc., feature structural stiffness and mass features, suitable for most of automotive/aerospace applications. In special, the low mass of these structures make them to be important acoustic radiators when excited by either structural or acoustic inputs. One way of reducing the motion of these structural members comes through the inclusion of small attachments to the structural host, thus realizing a structural MM, such that certain waves are prevented to propagate within the host. While this approach may find restrictions due to the mass addition of the attachments itself, this research shows that the inclusion of thermoplastic-based cells onto the lightweight host has a significant, localized impact on the STL of the host structural member, while keeping the overall mass impact as little as possible.

2.1 Numerical vibroacoustic approach

Beams are slender structural members that exhibit one dimension (length) predominantly larger than the other two dimensions (width and thickness). When subjected to low-frequency, dynamical transversal loads, flexural waves propagate unidirectionally among the ends of the structure. When excited around a flexural resonance, the beam will exhibit large dynamical displacements that cause the environment pressure to undergo significant oscillations, thus causing longitudinal, i.e. acoustic, waves in the surrounding fluid. Then, it is expected that the STL property of the unidimensional structure improves as the displacements of the material points are reduced. One technique to accomplish this consists on attaching a single vibration absorber, which can be tuned to either the resonance or frequency of interest. MM theories expand this concept, in which arrangements of resonant sub-systems are distributed onto a structure, which is currently known to create frequency gaps at which mechanical waves do not propagate. In this way, the STL of a bandwidth, rather than a single frequency, can be improved.

A numerical model can be conceived to study the transmission loss properties of a structure, based on finite and boundary element (FE-BE) methods. Then, a coupled FE-BE formulation can be invoked to study the scattering of the acoustic pressure of a structural member, in which the flexible modes are determined by discretizing the structure with finite elements, and the resulting acoustic pressure field at the exterior of the structural domain with boundary elements. The present problem can be mathematically hypothesized as follows (Atalla and Sgard, 2015):

$$\begin{bmatrix} (K-\omega^2 M) & C_{up} \\ -\rho_0\omega^2\mathscr{B}(\omega) & \mathscr{A}(\omega) \end{bmatrix} \begin{Bmatrix} u \\ p \end{Bmatrix} = \begin{Bmatrix} F \\ P \end{Bmatrix}, \tag{1}$$

where $\{K,\ M\} \in \mathbb{R}^{n_s \times n_s}$ stand for the structural stiffness and mass matrices respectively, discretized in n_s DoF; matrices $\{\mathscr{A},\ \mathscr{B}\}$ come from solving the nonhomogeneous (forced) acoustic wave equation by using the $2D$ Green function (matrix $\mathscr{A} \in \mathbb{R}^{n_p \times n_p}$ and matrix $\mathscr{B} \in \mathbb{R}^{n_p \times n_s}$); $C_{up} \in \mathbb{R}^{n_s \times n_p}$ represents the vibroacoustic coupling term; and terms F and P represent the external structural forcing and input acoustic pressure, respectively.

The model above described can be slightly modified to study the influence of an upstream pressure field that arrives at one side of the structure under study, on the pressure field generated on the opposite side of the beam as a result of its dynamical behavior. In this situation, the input excitation is no longer a structural force, so the term F in Eq. 1 becomes zero. Furthermore, the structure under study can be fixed in a hypothetical infinite baffled configuration, so that the acoustic field generated on the opposie side of the beam is not affected by the acoustic field directly generated by the source. In this way, the STL of the 1D structure can be properly studied.

Figure 1 illustrates the numerical model and vibroacoustic results obtained by using commercial software COMSOL. Parameters for the numerical model are given in Table 1.The frequency bandwidth of interest is $20-570$ Hz, in which three high-amplitude resonances can be clearly identified (*c.f.* Fig. 1(a)). For the purposes of this study, the second resonance of the bare structure at 235 Hz is targeted with the application of multiple resonant cells (*c.f.* Fig. 1(b)). Moreover, as the following sections will show, the resulting band gap covers a wide frequency band, starting from 170 Hz, and extending up to 240 Hz. In addition, the measuring points, P2 and P10, will be used to compare the transmissibility across the structure. In numerical analysis they will be referred as H11 and H21 respectively.

2.2 Numerical electromechanical approach

Automotive/aerospace applications often demand smart, adaptive devices and structures. In line with this need, the proposed acoustic metastructure is combined with piezoelectric attachments that are known for being both cheap and

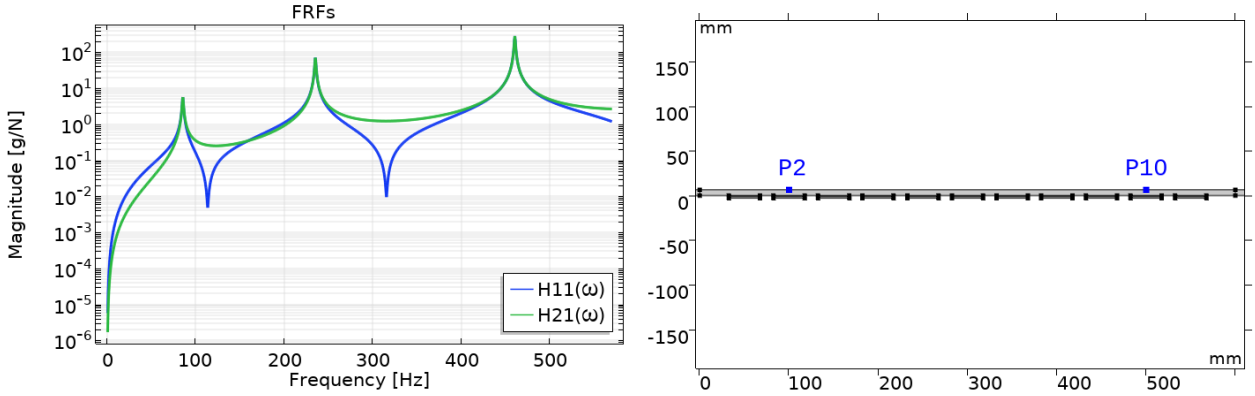

(a) (b)

Figure 1: (a) COMSOL model of the proposed AMM; (b) Numerical mechanical FRFs (H_{11} and H_{21}).

Table 1: Geometrical and material parameters for COMSOL simulations.

Parameter	**Value**	**Parameter**	**Value**
Length host	600[mm]	Young's modulus host	62[GPa]
Width host	25.4[mm]	Poisson's ratio host	0.3
Thickness host	6.35[mm]	Young's modulus ABS	1980[MPa]
Length attachment	35[mm]	Density ABS	1025.1[kg/m^3]
Thickness piezo	0.75[mm]	Poisson's ratio ABS	0.4
Thickness ABS	2[mm]	Damping host: α	7.5[s^{-1}]
Total thickness attachment	3.15[mm]	Damping host: β	1e-12[s]
Density host	2800[kg/m^3]	Spring attachments	25[kN/m]
		Damping attachments	0.75[Ns/m]

lightweight, which have been connected to shunt circuitry in order to provide the proposed device with adaptive properties.

The numerical coupling between structural, piezoelectric and shunt circuitry is mathematically formulated as follows (Zhou *et al.*, 2016; Silva *et al.*, 2018):

$$\begin{bmatrix} M & 0 \\ 0 & L \end{bmatrix} \begin{Bmatrix} \ddot{\vec{U}} \\ \ddot{q} \end{Bmatrix} + \begin{bmatrix} C & 0 \\ 0 & R \end{bmatrix} \begin{Bmatrix} \dot{\vec{U}} \\ \dot{q} \end{Bmatrix} + \begin{bmatrix} K_{SC} + \theta C_p^{-1} \theta^T & \theta C_p^{-1} \\ C_p^{-1} \theta^T & C_p \end{bmatrix} \begin{Bmatrix} \vec{U} \\ q \end{Bmatrix} = \begin{Bmatrix} F \\ 0 \end{Bmatrix}, \tag{2}$$

where $\{R,\ L\}$ are the resistor and inductor in the shunt circuit, respectively, matrix $C = \alpha M + \beta K$ is the host damping, assumed to be proportional to the mass matrix and short-circuit stiffness matrix, K_{SC}; θ stands for the electromechanical coupling term; C_p stands for the electrical stiffness term, *i.e.* the inherent piezoelectric capacitance, and the chosen degrees of freedom are the structural displacements (in x and y directions) and the electrical charge, q. While the experimental capacitance of the PZT-5A-based piezoelectric attachments was measured as $C_p = 25.25[nF]$, the one determined by using COMSOL software is $C_p = 31.01[nF]$, *i.e.* there is good agreement between numerical and experimental electromechanical approaches. It is worth noticing that, while COMSOL software uses structural solid elements to couple with piezoelectric materials, other computationally light and more suitable approaches to the problem at hand (electromechanical structures in bending motion) are available in the literature, *e.g.* electromechanical beams (Lumentut and Howard, 2014), plates (De Marqui Jr. *et al.*, 2009), shells (Loghmani *et al.*, 2017)), which allow the realization of the calculations in a faster, but still accurate way. Notice also that, in Eq. 2, vector $\vec{U} \in \mathbb{R}^2 = [u,\ v]^T$ denotes the local displacement coordinates for a given structural point (2D solid).

In a previous effort (Rodrigues *et al.*, 2019), the modular modeling process of the unit cell with electromechanical coupling has been addressed. A computationally tractable metamodel of the cells has been conceived, mainly focused on their electromechanical behavior. As Fig. 2 illustrates, each attachment is considered to be a layered system, featuring a piezo patch (in dark gray) sandwiched between two layers of thermoplastic ABS material (light gray). This approach attempts to recreate the electromechanical effect of the piezoelectric material on the MM. The cells are then attached to the host structure via spring elements, which is seen to reproduce the effect of the actual attachments to the host. As pointed in (Rodrigues *et al.*, 2019), the behavior of the thermoplastic scatters over a range due to manufacturing process. This can be seen later on this paper as the band gap zone of the mechanical response of the MM exhibit multiple dips indicating multiples resonant frequencies of the cells.

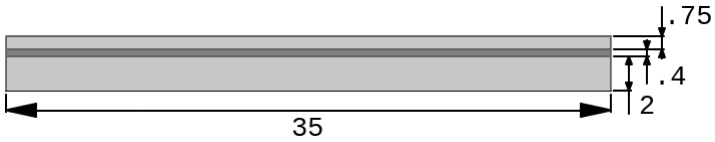

Figure 2: FEM geometry of the resonator cell

Then, a vibroacoustic analysis recreate the condition for sound suppression in a open field. For the sound source, a monopole oscilating at 200 Hz at 1 Pa is placed at the underside of the structure off-centered seeking the excitation of both even and odd structural modes. One can easily see that in center excitation would promote a cancel for even structural modes as they are anti symmetrical to the center point. As mentioned beforehand, an infinite baffle is settled to isolate the incident side and the radiated side to prevent the wave bending. A pressure field in a target frequency, which may be on the rejection band created by the cells, is taken as the result of the simulation and the responses of the bare structure and the smart metastructure will be compared. Further research will be develop for evaluation of the sound irradiation from the structures, both bare and treated, due to a mechanical excitation and also the Sound Transmission Loss in a wider frequency band aiming also for the side peaks of the band gap as they are targeted with the resonant shunt.

3. RESULTS

Experimental analyses were carried out on a clamped-clamped 1D structure, *c.f.* Fig. 3. Transverse vibrations have been induced with the aid of an electrodynamical shaker, in P2, and the structural wave propagation was measured with accelerometers mounted across the structure. A modal analysis was carried out in order to compare the responses from different MM setups: the bare 1D structure, the LRMM and the LRSMM.

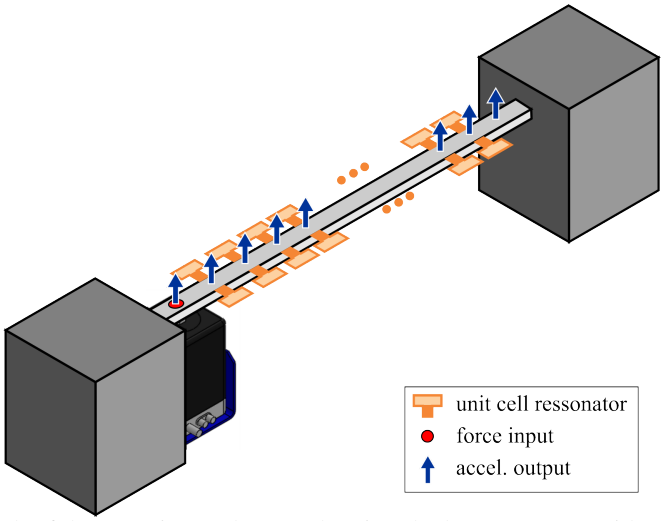

Figure 3: Sketch of the experimental setup showing the host structure with no attachments.

Current results of the proposed device show a band gap that tackles the second structural mode, *c.f.* Fig. 4. In this Figure, one can observe that the mass addition to the structure causes the first and third resonances to be shifted down in frequency, and this effect has been considered in the cell design. With regard to the size of the MM actuation band, the experimentally observed bandgap is notably 100Hz wide and still exhibits a significant intensity, yet lower than the obtained one by common LRMMs. Moreover, while the numerical model does also reproduce the effect of the spatially distributed attachments along the structure, *c.f.* Fig. 5(a) and (b), the width of the obtained bandgap is quite short, although it is more pronounced than the experimental one, see Fig. 5(b) that illustrates a FRF between the excitation point and a measurement point far from the excitation one. At this point, the numerical model gives valuable insights on the causes of such bandgap behaviors (width and deepness/intensity), since the numerical model has considered equal structural properties for all of the attachments, and also the same spring connector (adhesive layer) for all the attachments. Hence, one could state that the main reason for these bandgap results is given by variations in the geometrical and physical parameters among the mechanical resonators that result from the fabrication processes.

Moreover, the inclusion of a piezoelectric attachment in the form of a tuned shunt circuitry has noticeably improved the performance, attaining 18dB of amplitude reduction at the higher frequency peak that naturally appears on the gap border, *c.f.* Fig. 4. This effect has been successfully reproduced by using resistor-inductor shunt circuits in the numerical models, as it can be seen in Fig. 5. The numerical simulations have considered optimal resistance values, which have been

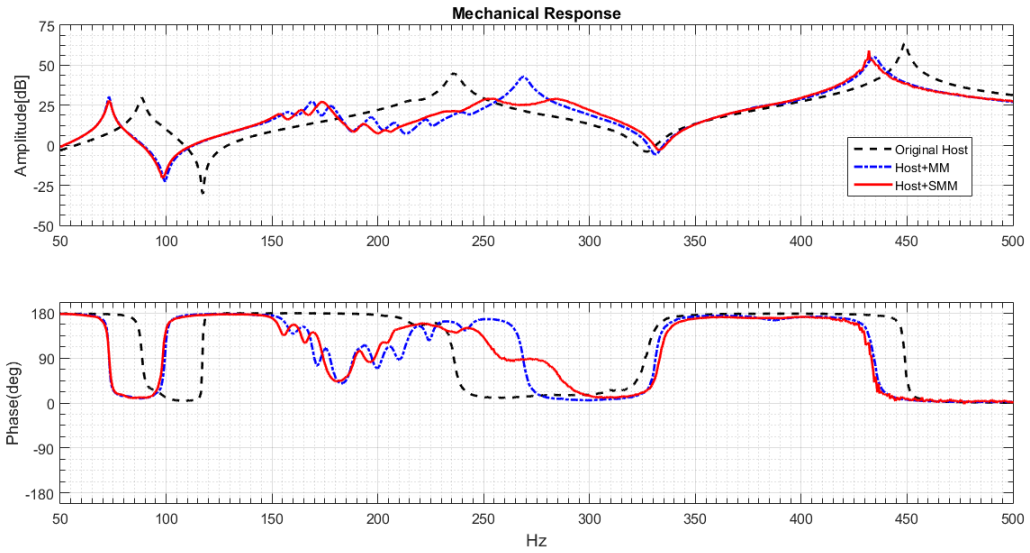

Figure 4: Comparison between experimental frequency response functions.

calculated in the following way (Yamada *et al.*, 2010):

$$Rc = \sqrt{\frac{3}{2}}\left(\frac{K_c}{\omega_{OC}(2)Cp}\right), \tag{3}$$

where $\omega_{OC}(2)$ is the second open-circuit electromechanical resonance, Cp is the inherent piezoelectric capacitance, and Kc is the modal electromechanical coupling, which is calculated as follows:

$$Kc = \sqrt{\frac{\omega_{OC}(2)^2 - \omega_{SC}(2)^2}{\omega_{OC}(2)^2}}, \tag{4}$$

where $\omega_{SC}(2)$ is the second short-circuit electromechanical resonance. Surprisingly enough, the numerical resistance value equals $1.9k\Omega$, whereas the actual real impedance value of the synthetic inductors is $1.0k\Omega$.

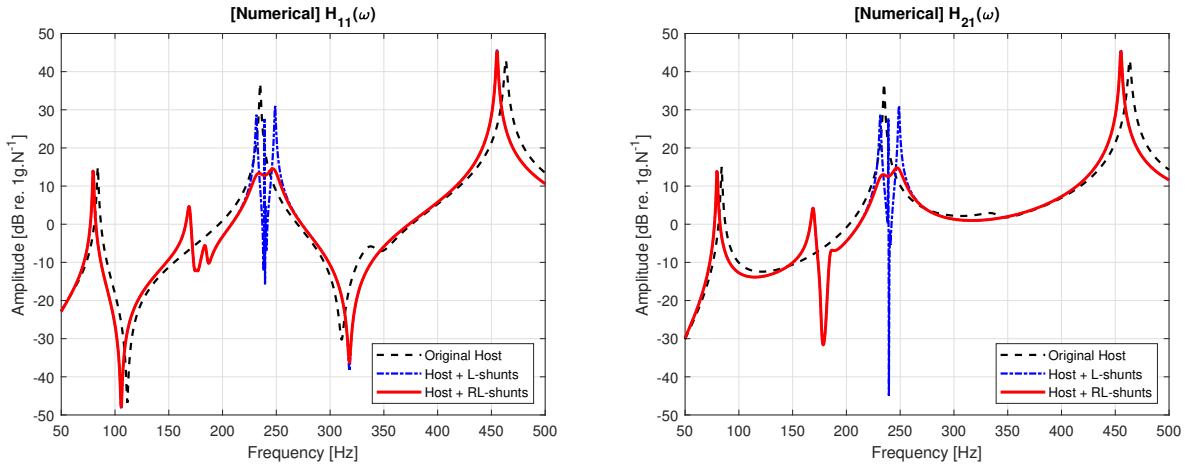

(a) (b)

Figure 5: Comparison between numerical frequency response functions: (a) H_{11}; (b) H_{21}.

The sound pressure level distribution for a single excitation frequency at 200 Hz has been numerically assessed, before (*c.f.* Fig. 1) and after the implementation of the proposed MM, *c.f.* Fig. 6. The visual comparison of the distributions reveal that, while the bare structure yields a resulting SPL distribution of around 55 dBSPL at the opposite side of the beam, the one provided with the proposed piezoelectric attachments reduced the resulting sound field in around 15 dB, thus yielding an overall SPL of 40 - 45dBSPL. This promissory numerical insight can be confirmed through the experimental results,

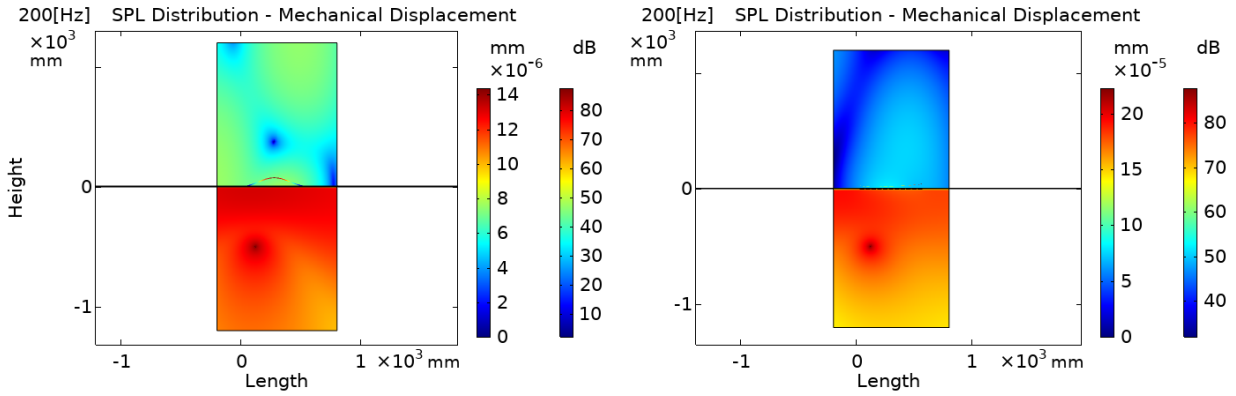

(a) (b)

Figure 6: Numerical result of the spatial distribution of the sound pressure level: (a) bare beam; (b) proposed MM device.

since the electromechanical results from both numerical and experimental campaigns agree well to each other, *c.f.* Figs. 4 and 5.

Figure 7 confirms that the structural transmissibility has been hindered around the gap zone. This effect indicates that waves whose frequency match the bandgap ones will be attenuated, if trying to propagate within the structure.

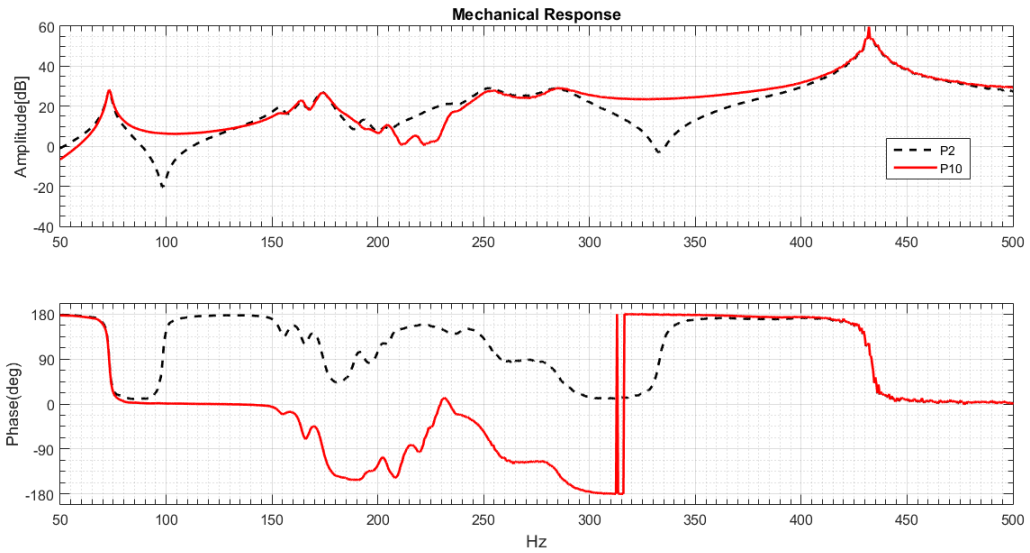

Figure 7: Frequency response in symmetric opposites

4. CONCLUSIONS

This paper has presented a unidimensional acoustic metamaterial with enhanced sound transmission loss features and adaptive capabilities. Numerical approaches, *e.g.* finite elements for electromechanical domains, and boundary elements for acoustic domains, have been used and coupled in the aim of studying the acoustic radiation of the proposed 1D metastructure when loaded by acoustic excitations. The adaptive electromechanical metastructure has been built with lightweight materials, *e.g.* aluminium for the host, and thermoplastic ABS and piezoelectric PZT-5A material for the attachments, and experiments have been run in order to identify the effect of the attachments on the dynamic behavior of the bare structure and the on acoustic radiation.

As the experimental results have revealed, significant vibration suppression of transverse waves traveling across the structure is feasible thanks to the spatial distribution of the proposed electromechanical LR (locally resonant) unit cells. The transmissibility across the structure is seen to be reduced by the LRMM, and the addition of the piezo disks, combined with shunt circuitry, has yielded in an extra band control zone with significant actuation. Therefore, the experimental data demonstrate that the proposed locally resonant, shunted acoustic metamaterial is promissory for sound insulation applications, since the low-frequency, high-power structural resonances can be notably and robustly attenuated, with little

impact on the overall mass of the realized smart metamaterial, as well as with the addition of synthesized inductors that can be tuned according to the demands of a given aerospace/automotive application.

5. ACKNOWLEDGEMENTS

The authors acknowledge the financial support of the Brazilian National Council for Scientific and Technological Development - CNPq, grant number 302486/2018-6 and the scholarship awarded to the first author, as well as the support from the São Paulo Research Foundation - FAPESP, through the grants nr. 2018/15894-0 and 2018/14546-9.

6. REFERENCES

Atalla, N. and Sgard, F., 2015. *Finite Element and Boundary Methods in Structural Acoustics and Vibration*. CRC Press.

De Marqui Jr., C., Erturk, A. and Inman, D.J., 2009. "An electromechanical finite element model for piezoelectric energy harvester plates". *Journal of Sound and Vibration*, Vol. 327, pp. 9–25.

De Oliveira, L., Da Silva, M.M., Sas, P., Van Brussel, H. and Desmet, W., 2008. "Concurrent mechatronic design approach for active control of cavity noise". *Journal of Sound and Vibration*, Vol. 314, No. 3-5, pp. 507–525.

Douglas, B. and Yang, J., 1978. "Transverse compressional damping in the vibratory response of elastic-viscoelastic-elastic beams". *AIAA journal*, Vol. 16, No. 9, pp. 925–930.

Dovstam, K., 1995. "Augmented hooke's law in frequency domain. a three dimensional, material damping formulation". *International Journal of Solids and Structures*, Vol. 32, No. 19, pp. 2835–2852.

Inman, D.J. and Singh, R.C., 1994. *Engineering vibration*, Vol. 3. Prentice Hall Englewood Cliffs, NJ.

Li, J., Zhou, X., Huang, G. and Hu, G., 2016. "Acoustic metamaterials capable of both sound insulation and energy harvesting". *Smart Materials and Structures*, Vol. 25, No. 4, p. 045013.

Loghmani, A., Danesh, M., Kwak, M.K. and Keshmiri, M., 2017. "Vibration suppresion of a piezo-equipped cylindrical shell in a broad-band frequency domain". *Journal of Sound and Vibration*, Vol. 411, pp. 260–277.

Lumentut, M.F. and Howard, I.M., 2014. "Electromechanical finite element modelling for dynamic analysis of a cantilevered piezoelectric energy harverster with tip mass offset under base excitations". *Smart Materials and Structures*, Vol. 23, pp. 095037, 24pp.

Mosquera-Sánchez, J.A., Desmet, W. and de Oliveira, L.P.R., 2017. "A multichannel amplitude and relative-phase controller for active sound quality control". *Mechanical Systems and Signal Processing*, Vol. 88, pp. 145–165.

Rodrigues, G.K., da Silva, M.M. and de Oliveira, L.P.R., 2019. "Modular modeling approach for FDM printed structures and piezo disks for metamaterial design". *Latin American Journal of Solids and Structures*. doi:10.1590/1679-78255310.

Silva, T., Clementino, M.A., C., D.M.J. and A., E., 2018. "An experimentally validated piezoelectric nonlinear energy sink for wideband vibration attenuation". *Journal of Sound and Vibration*, Vol. 437, pp. 68–78.

Yamada, K., Matsuhida, H., Utsuno, H. and Sawada, K., 2010. "Optimum tuning of series and parallel LR circuits for passive vibration suppression using piezoelectric elements". *Journal of Sound and Vibration*, Vol. 329, pp. 5036–5057.

Zhou, B., Zang, C. and Wang, X., 2016. "Exploration of nonlinearly shunted piezoelectrics as vibration absorbers". *Journal of Physics: Conference Series*, Vol. 744, pp. 012120, 12pp.